Journal of
Plankton Research

academic.oup.com/plankt

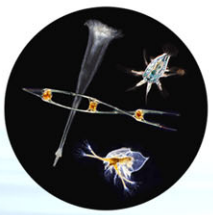

J. Plankton Res. (2017) 39(3): 423–435. *First published online April 13, 2017 doi:10.1093/plankt/fbx017*

Spatial and seasonal distributions of photosynthetic picoeukaryotes along an estuary to basin transect in the northern South China Sea

WENXUE WU[1,2], LEI WANG[1,2,3], YU LIAO[1,2], SONGLI XU[1,2] AND BANGQIN HUANG[1,2]*

[1]KEY LABORATORY OF COASTAL AND WETLAND ECOSYSTEMS, XIAMEN UNIVERSITY, XIAMEN 361102, CHINA, [2]STATE KEY LABORATORY OF MARINE ENVIRONMENTAL SCIENCE, XIAMEN UNIVERSITY, XIAMEN 361102, CHINA AND [3]THIRD INSTITUTE OF OCEANOGRAPHY, STATE OCEANIC ADMINISTRATION, XIAMEN 361005, CHINA

*CORRESPONDING AUTHOR: bqhuang@xmu.edu.cn

Received August 3, 2016; editorial decision March 19, 2017; accepted April 1, 2017

Corresponding editor: John Dolan

The spatial and seasonal distributions of marine photosynthetic picoeukaryotes (PPEs) and the underlying structuring mechanisms are not well understood. Here, we performed Fluorescent *in situ* hybridization associated with tyramide signal amplification along an estuary to basin transect in the northern South China Sea (SCS) across three seasons (spring, summer and autumn). We disentangled the PPE assemblage variances by combining these data with the results obtained in our previous study conducted in winter to evaluate the relative importance of environmental, spatial and temporal effects. Our results showed that Mamiellophyceae was the most abundant class and accounted for an average of 33.1% (spring), 34.2% (summer) and 30% (autumn) of the depth-integrated picoeukaryotic abundances in different seasons. Prymnesiophyceae species were widely detected across the three seasons, and Pelagophyceae species were remarkably abundant in the chlorophyll maximum depth in summer. Bolidophyceae represents an important PPE class and made considerable contributions (up to 25.4% in autumn) to the depth-integrated picoeukaryotic abundances. Moreover, the PPE assemblages were significantly explained by purely environmental (6.5%) and purely temporal (42.7%) components, and they were also explained by a weak and non-significant spatial component (1.9%). In summary, our results provide insights into PPE distributions that are differently influenced by environmental, spatial and temporal components in the northern SCS.

KEYWORDS: FISH-TSA; mamiellophyceae; prymnesiophyceae; pelagophyceae; bolidophyceae; metacommunity; variation partitioning

available online at academic.oup.com/plankt

INTRODUCTION

Photosynthetic picoeukaryotes (PPEs, nominally defined as cells <3 μm in diameter) are vital components of marine ecosystems (Vaulot *et al.*, 2008). PPE assemblages have been shown to dominate plankton biomass (Worden *et al.*, 2004; Grob *et al.*, 2007; Cuvelier *et al.*, 2010) and primary production (Li, 1994; Morán, 2007; Jardillier *et al.*, 2010) in coastal waters and open oceans. Recent advances have significantly expanded our knowledge of the ecological roles of PPEs by showing that these organisms are important consumers of bacteria and have the potential to act as the dominant bacterivores in an ecosystem (Zubkov and Tarran, 2008; Hartmann *et al.*, 2012; McKie-Krisberg and Sanders, 2014). PPEs exhibit astonishing diversity as revealed by molecular surveys based on sequencing and analyses of plastid-encoded 16S rRNA (Fuller *et al.*, 2006a; Lepère *et al.*, 2009; Shi *et al.*, 2011; Kirkham *et al.*, 2011a, b) and 18S rRNA genes (Moon-van der Staay *et al.*, 2001; Shi *et al.*, 2009); however, PPE assemblages from filtered samples without cell sorting are typically outnumbered by heterotrophs (Marie *et al.*, 2010). The tremendous diversity of PPEs may translate into distinct resource utilization strategies and traits among clades and species that regulate fundamental PPE functions in marine ecosystems (Bonachela *et al.*, 2016).

Qualitative and quantitative evaluations of PPE distributions (i.e. compositions and amounts) are core measurements for determining their ecological roles in ecosystem functioning. A series of approaches have been developed to determine the composition and abundance of PPEs. Pigment analyses based on high-performance liquid chromatography represent a common approach used in early studies designed to ascertain the relative biomass contributions among major PPE groups (Millie *et al.*, 1993; Blanchot *et al.*, 2001), and dot blot hybridization technology that targets plastid 16S rRNA gene amplicons has also been used in several studies (Fuller *et al.*, 2006b; Lepère *et al.*, 2009; Kirkham *et al.*, 2011a, b, 2013; Bouman *et al.*, 2012). Nevertheless, pigment analyses and dot blot hybridization technology resolve PPE distributions and compositions based on relative contributions but omit abundance information (i.e. cell number). Fluorescent *in situ* hybridization associated with tyramide signal amplification (FISH-TSA) provides a robust approach that yields taxonomic PPE abundances (Not *et al.*, 2002; Biegala *et al.*, 2003). Using FISH-TSA, PPE assemblages have been investigated in many regions over the past decade (Not *et al.*, 2008; Grob *et al.*, 2011; Kirkham *et al.*, 2011a; Wu *et al.*, 2014b; Cabello *et al.*, 2016). The main result based on these various approaches appears to suggest that four groups, Chlorophyta, Prymnesiophyceae, Pelagophyceae and Chrysophyceae, account for the major proportion of PPE diversity, biomass and abundance. However, the importance of each group varies greatly in different regions that have spatially heterogeneous environments. For instance, although Chrysophyceae species were found to dominate the PPE assemblages along a pelagic transect in the Atlantic Ocean (Kirkham *et al.*, 2011b), they were not detected at coastal sites in the northeastern Atlantic Ocean (Cabello *et al.*, 2016). Moreover, Ho *et al.* (2015) found that Chrysophyceae did not represent a dominant group in the northern South China Sea (SCS) based on seasonal pigment surveys at a basin scale.

To understand the distribution patterns of PPEs, the underlying mechanisms shaping PPE assemblages must be determined. According to the metacommunity context (Leibold *et al.*, 2004), ecological communities are mainly regulated by two categories of ecological processes: niche-related effects (hereafter environmental filtering) versus neutral effects (hereafter dispersal limitation). A metacommunity is defined as a set of local communities that contain potentially interacting taxa linked by dispersal within a region (Leibold *et al.*, 2004). Environmental filtering shows the role of local environmental heterogeneities associated with distinct niches of taxa, whereas dispersal limitations indicate the degree of difficulty associated with the dispersal of organisms from one patch to another. Reports have indicated that phytoplankton assemblages are structured either exclusively by environmental variations (Vanormelingen *et al.*, 2008; Huszar *et al.*, 2015) or spatial distances (Vyverman *et al.*, 2007) as well as by both factors (De Bie *et al.*, 2012). For PPEs, the environmental parameters (e.g. temperature and nutrients) contribute to their composition from a global perspective (Kirkham *et al.*, 2013). Compared with the role of environmental variations (which are commonly illustrated by ordination plots), the relative importance of spatial distances is poorly understood (Hamilton *et al.*, 2008). Overall, despite contrasting PPE distribution patterns in marine environments, the driving forces remain controversial.

The SCS is a large marginal sea located in the northwestern Pacific Ocean. The northern SCS is influenced by a series of oceanographic processes driven by seasonal East Asian monsoons (Hu *et al.*, 2000). More specifically, the hydrographic conditions in the northern SCS show a clear stratification in spring and summer but are well mixed in autumn and winter. PPE spatial distributions have been reported in the northern SCS in winter (Wu *et al.*, 2014b), whereas seasonal variations of abundance-based PPE distributions remain unavailable. Insufficient background information is available on the seasonal distributions of PPEs, which limits our understanding of PPE assemblages in the northern SCS and

their capacity to respond to environmental variations (Treusch *et al.*, 2012; Mouriño-Carballido *et al.*, 2016). The first aim of this work is to determine the seasonal PPE compositions and abundances in the northern SCS. We performed FISH-TSA across three seasons (spring, summer and autumn) along the same transect used in Wu *et al.* (2014b), which extends from the Pearl River Estuary to the SouthEast Asia Time-series Study (SEATS) station. Thus, our second aim is to isolate the relative importance of environmental filtering, dispersal limitations and temporal effects in the structuring of PPE assemblages.

METHOD

Sample collections

Samples were repeatedly collected at 10–12 stations extending from the Pearl River Estuary to the SEATS station during three cruises (autumn, November 2010; spring, May 2011; and summer, July–August 2012; Fig. 1). The vertical temperature and salinity profiles were obtained using casts equipped with an SBE-911 CTD (Sea-Bird Electronics, USA). Seawater was sampled on board using 20 L Niskin bottles mounted on a rosette. A total of 2–6 samples were collected at each station at depths of 0–150 m for the FISH-TSA analysis and nutrient and chlorophyll *a* (Chl *a*) measurements.

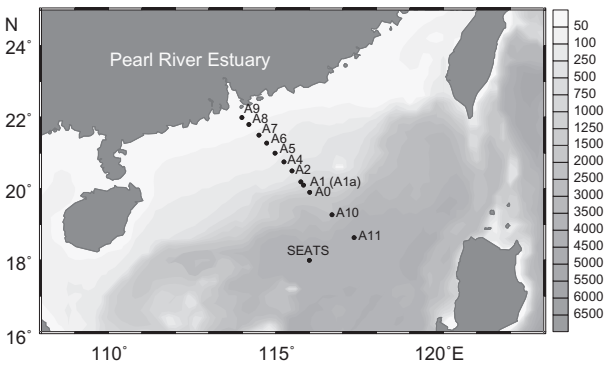

Fig. 1. Sampling locations in the northern SCS. Black dots on the map correspond to the 13 sampling stations of the three cruises. For each cruise, 10–12 stations were sampled. Gray contours represent the bottom depth (m), and the scale is at the sidebar. The map plots were generated using the Ocean Data View program (Schlitzer, 2011).

For the FISH-TSA analysis, seawater samples of 75–200 mL were pre-filtered through 3 μm pore polycarbonate filters (Millipore, USA). The filtrate samples were immediately fixed in PBS-buffered paraformaldehyde (Sigma-Aldrich, USA, 1% final concentration) for 1 h at room temperature. The fixed cells were collected using 0.2 μm pore polycarbonate filters under 200 mmHg pressure. A serial dehydration was performed using an ethanol series of 50, 80 and 100% (3 min each). The dehydrated samples were then transported back to the laboratory and stored at −80°C until analysis.

Fluorescent *in situ* hybridization associated with tyramide signal amplification

To determine the total number of picoeukaryotic cells, we used a combination of the EUK1209, CHL01 and NCHL01 probes (Not *et al.*, 2008) labeled with horseradish peroxidase (Thermo Fisher Scientific, Germany) (Table I). We used the CHL02, PRYM02 and PELA01 probes to target three potentially major groups: Chlorophyta, Prymnesiophyceae and Pelagophyceae. Our results indicate that Chlorophyta, particularly Mamiellophyceae, dominate the PPE abundances in the northern SCS in winter (Wu *et al.*, 2014b). As a result, we focused on Chlorophyta by using a probe set that included PRAS04, MICRO01, OSTREO01 and BATHY01, which are specific for Mamiellophyceae, *Micromonas*, *Ostreococcus* and *Bathycoccus*, respectively. Moreover, minor PPE groups, such as Bolidophyceae, were not considered in previous studies (with the exception of Not *et al.*, 2005 and Piwosz *et al.*, 2015) because of the low throughput of FISH-TSA. Although Bolidophyceae species are widely distributed from equatorial to polar waters (Guillou, 2011; Ichinomiya

Table I: List of oligonucleotide probes used in this study

Probe	Sequence (5′–3′)	Target groups	Reference
EUK1209R	GGG CAT CAC AGA CCT G	Eukaryotes	Giovannoni *et al.* (1988)
CHLO01	GCT CCA CGC CTG GTG GTG	Chlorophyta	Simon *et al.* (1995)
NCHLO01	GCT CCA CTC CTG GTG GTG	Non-Chlorophyta	Simon *et al.* (1995)
CHLO02	CTT CGA GCC CCC AAC TTT	Chlorophyta	Simon *et al.* (2000)
PRYM02	GGA ATA CGA GTG CCC CTG AC	Prymnesiophyceae	Simon *et al.* (2000)
PELA01	ACG TCC TTG TTC GAC GCT	Pelagophyceae	Simon *et al.* (2000)
BOLI02	TAC CTA GGT ACG CAA ACC	Bolidophyceae	Guillou *et al.* (1999)
PRAS04	CGT AAG CCC GCT TTG AAC	Mamiellophyceae	Not *et al.* (2004)
MICRO01	AAT GGA ACA CCG CCG GCG	*Micromonas*	Not *et al.* (2004)
OSTREO01	CCT CCT CAC CAG GAA GCT	*Ostreococcus*	Not *et al.* (2004)
BATHY01	ACT CCA TGT CTC AGC GTT	*Bathycoccus*	Not *et al.* (2004)

et al., 2016), their seasonal distribution in the SCS remains unclear. To achieve a comprehensive perspective, we assessed the distribution of Bolidophyceae using the specific probe BOLI02.

The FISH-TSA analysis was performed (Not *et al.*, 2002) by incubating each filter for 3 h at 35°C with a mixture of 2 μL of the probe (50 ng μL^{-1}) and 18 μL of the hybridization buffer, which consisted of 40% deionized formamide (Sigma-Aldrich, USA), 0.01% (w/v) sodium dodecyl sulfate (SDS, Sigma-Aldrich, USA), 0.9 M NaCl, 20 mM Tris-HCl pH 7.5 and 2% blocking reagent (Roche, Germany). The samples were then washed twice for 20 min at 37°C in preheated washing buffer (56 mM NaCl, 5 mM EDTA, 0.01% SDS and 20 mM Tris-HCl pH 7.5). Prior to the TSA reaction, the filters were equilibrated for 15 min at room temperature in TNT buffer (100 mM Tris-HCl pH 7.5, 150 mM NaCl, 0.07% (v/v) Tween 20). For the TSA reaction, filter pieces were transferred to 1 mL of the amplification buffer (1.6 M NaCl, 0.08% blocking reagent, 0.8 × PBS pH 7.6, 8% dextran sulfate), to which H_2O_2 at a final concentration of 0.001% (w/v) and 10 μL of tyramides labeled with Alexa-488 (1 mg mL^{-1}) (Molecular Probes, USA) were added. The TSA reactions were performed in the dark for 30 min at room temperature. The filters were then washed twice in TNT buffer at 55°C for 20 min each, briefly rinsed in Milli-Q water, and then air dried. Finally, the filter sections were counterstained with a 20 μL mixture of 4′,6-diamidino-2-phenylindole (Sigma-Aldrich; 5 μg mL^{-1} final concentration) in antifading solution (10:2:1 (v/v/v), glycerol:AF3 (Citifluor, UK): 20 × PBS). All of the filter pieces were observed under an Eclipse 90i fluorescence microscope (Nikon, Japan). Over 20 randomly chosen fields of view were counted along several transects on the filter.

Environmental variables

Nutrient samples were collected and analyzed on board using a Technicon AA3 Auto-Analyzer (Bran-Lube, Germany) as described in Du *et al.* (2013). The samples for the total Chl *a* measurements were filtered directly onto GF/F filters without pre-filtering and determined on board using a Trilogy Fluorometer (Turner Designs, USA) as described in Wu *et al.* (2014b).

Data analysis

To compare the PPE compositions across spatial and seasonal scales, we used depth-integrated abundances for each group at each station. Statistical analyses using depth-integrated data provide site-based comparisons that group the effects of vertical mixing related to environmental and spatial factors. Nevertheless, depth-integrated data may also hide the vertical dimension of the relative importance of environmental and spatial factors because environmental and spatial forces shaping PPE assemblage structures may vary at different depths. These results were combined with a previous survey conducted on the same transect in winter (Wu *et al.*, 2014b). We performed a nonmetric multidimensional scaling analysis (NMDS) and an analysis of similarity (ANOSIM) using the vegan package (Oksanen *et al.*, 2014).

To determine the fraction of variation explained by the environmental (environmental filtering), spatial (dispersal limitation) and temporal (seasonality) factors, we performed a three-way permutational multivariate analysis of variance (PERMANOVA) (McArdle and Anderson, 2001). Variations in the depth-integrated PPE composition among the stations were quantified using the Bray–Curtis dissimilarity. To extract the environmental variability, we performed a principal components analysis for the depth-integrated variables, and the first three axes were used to represent the environmental heterogeneities according to the Kaiser–Guttman rule. To determine the spatial variability (the proxy of dispersal limitation), we used Moran's eigenvector map approach (MEM) with the PCNM package (Legendre *et al.*, 2013) based on the longitude and latitude coordinates. Furthermore, we considered all stations in each season to represent one metacommunity and assumed that the metacommunities in the four sampling seasons were influenced by temporal effects in addition to the quantified environmental filtering and dispersal limitations. The MEM was also performed according to the sampling season to represent the seasonal variability. The PERMANOVA was implemented following Yeh *et al.* (2015). The following six fractions were primarily identified as explaining the variations of PPE assemblages: the environmental component [E]; spatial component [S]; temporal component [T]; purely environmental component without spatial and seasonal counterparts [E|S + T]; purely spatial component without environmental and seasonal counterparts [S|E + T]; and purely temporal component without environmental and spatial counterparts [T|E + S]. The significance of each component except for the interaction component was evaluated with 999 permutations (Legendre, 2008). The data analyses were conducted in the R program (R Core Team, 2014).

RESULTS

Environmental factors

The spatial and seasonal environmental factors were explored along the transect during the three cruises. In

spring, the environmental conditions at coastal stations A9 and A8 were obviously different from those at the other stations. Specifically, the surface temperature and salinity along the transect displayed minima (25.4°C and 33.1) at Station A9 (Supplementary Fig. S1A–B), thus indicating the influence of freshwater. The surface water at Station A9 also exhibited the highest Chl *a* concentration (1.9 μg L^{-1}) (Supplementary Fig. S1C). In the surface layer, nitrate and nitrite (NO_2 + NO_3) showed concentrations of 3.2 and 0.3 μM at Stations A9 and A8, respectively, but were depleted at the other 10 stations (from Stations A7 to SEATS) (Supplementary Fig. S1D). However, the phosphate (PO_4) concentrations in the surface layers of Stations A9 and A8 were below the detection level (<0.1 μM) (Supplementary Fig. S1E). Silicate (SiO_3) exhibited generally homogenous distributions within the upper 25 m of the water column (Supplementary Fig. S1F). In summer, the environmental variables showed patterns similar to those observed in spring (Supplementary Fig. S1G–L). The stratified status of the hydrographic conditions in summer was stronger than that in spring and showed sharper gradients in the vertical profiles. Compared with the stratified conditions in spring and summer, the water columns in autumn were well-mixed down to 75 m (Supplementary Fig. S1M–R). For the shallow-depth stations A9 to A7, the nutrient (NO_2 + NO_3, PO_4 and SiO_3) profiles were remarkably homogenous from the surface to the bottom (Supplementary Fig. S1P–R). Overall, the hydrographic conditions showed obvious spatial and seasonal variations.

PPE distribution patterns

The PPE abundances exhibited large spatial and seasonal variations. In spring, the majority of PPE groups (Chlorophyta, Prymnesiophyceae, Bolidophyceae, Mamiellophyceae, *Ostreococcus* and *Bathycoccus*) reached their highest abundances at coastal station A9, which had a complete picoeukaryotic count of 9701 cells mL^{-1} (Supplementary Table S1 and Fig. 2AA–I). In summer, the PPE counts were highest mainly at the 50 m depth and exhibited a clear subsurface maximum layer (Supplementary Table S1 and Fig. 2BA–I). In autumn, the total picoeukaryotes presented a maximum of 18 426 cells m^{-1} at a depth of 5 m at Station A1 (Supplementary Table S1 and Fig. 2CA–I). However, many of the PPEs (Pelagophyceae, Bolidophyceae Mamiellophyceae, *Ostreococcus* and *Bathycoccus*) displayed their highest counts at nearby Station A2.

The depth-integrated abundances (Fig. 3) showed that the entire PPE assemblage was mainly composed of Chlorophyta (dominated by Mamiellophyceae, Supplementary Fig. S2), Prymnesiophyceae, Pelagophyceae and Bolidophyceae. Mamiellophyceae was the most important group and presented average relative contributions of 33.1, 34.2 and 30% in spring, summer and autumn, respectively (Fig. 3A, C and E). Prymnesiophyceae species were detected at all stations and presented average relative contributions of 16.8, 12.3 and 13.2% in spring, summer and autumn, respectively (Fig. 3A, C and E). Pelagophyceae exhibited significantly high proportions in summer that ranged from 13% (1039 cells mL^{-1}, Station A6) to 34.3% (1198 cells mL^{-1}, SEATS) (Fig. 3A, C and E). Bolidophyceae sporadically displayed high depth-integrated abundances and relative contributions ranging from 1.4% (28 cells mL^{-1}, Station A10, autumn) to 25.4% (724 cells mL^{-1}, Station A6, autumn) (Fig. 3E).

Ostreococcus and *Bathycoccus* accounted for most of the depth-integrated abundances of Mamiellophyceae in spring and summer. In spring, the depth-integrated abundances of *Bathycoccus* were slightly higher in spring than those of *Ostreococcus* (Fig. 3B), whereas *Ostreococcus* dominated the abundance of Mamiellophyceae in summer (Fig. 3D). In autumn, *Micromonas* showed considerable relative abundances in the coastal waters with a maximum of 56% at Station A9 (Fig. 3F). Notably, the counts of Mamiellophyceae in spring were generally less than the sum of the three genera (with the exception of Station A8), which indicated that the probe PRAS04 failed to target many of the cells of *Ostreococcus* and *Bathycoccus* in this season (Supplementary Fig. S3).

PPE assemblages and determinations

The NMDS plots showed that the PPE assemblages from each season were relatively clustered together, indicating seasonal variations in the PPE composition (Fig. 4). The seasonal variations of the PPE assemblages among the four seasons were significant ($P = 0.001$, permutations = 999) as indicated by the ANOSIM.

The depth-integrated PPE assemblages were significantly explained by the purely environmental (6.5%; $P < 0.05$) and seasonal (42.7%; $P < 0.05$) components, and the spatial component provided a weak explanation (1.9%; $P > 0.05$) (Fig. 5).

DISCUSSION

To the best of our knowledge, this is the first study to reveal the spatial and seasonal PPE assemblages based on the cell numbers along a fixed transect. Previous reports have determined the PPE abundances in several regions by employing FISH-TSA, and the results showed very

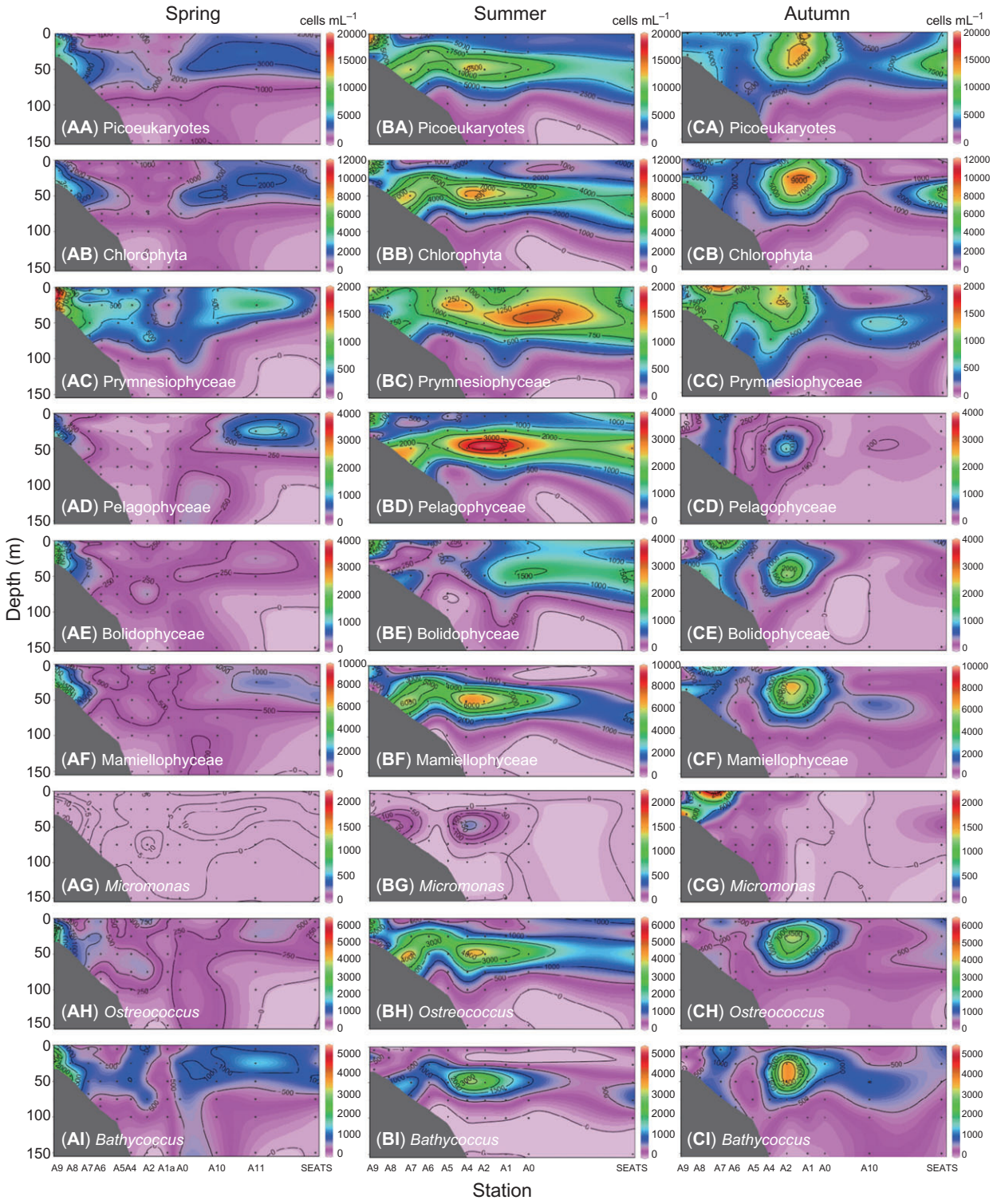

Fig. 2. Vertical and horizontal distribution of picoeukaryotes, Chlorophyta, Prymnesiophyceae, Pelagophyceae, Bolidophyceae, Mamiellophyceae, *Micromonas*, *Ostreococcus* and *Bathycoccus* (cells mL^{-1}) during the spring (**AA**–**I**; left), summer (**BA**–**I**; middle) and autumn (**CA**–**I**; right) cruises. Black dots correspond to the sampling points. Contour plots were generated using the Ocean Data View program (Schlitzer, 2011).

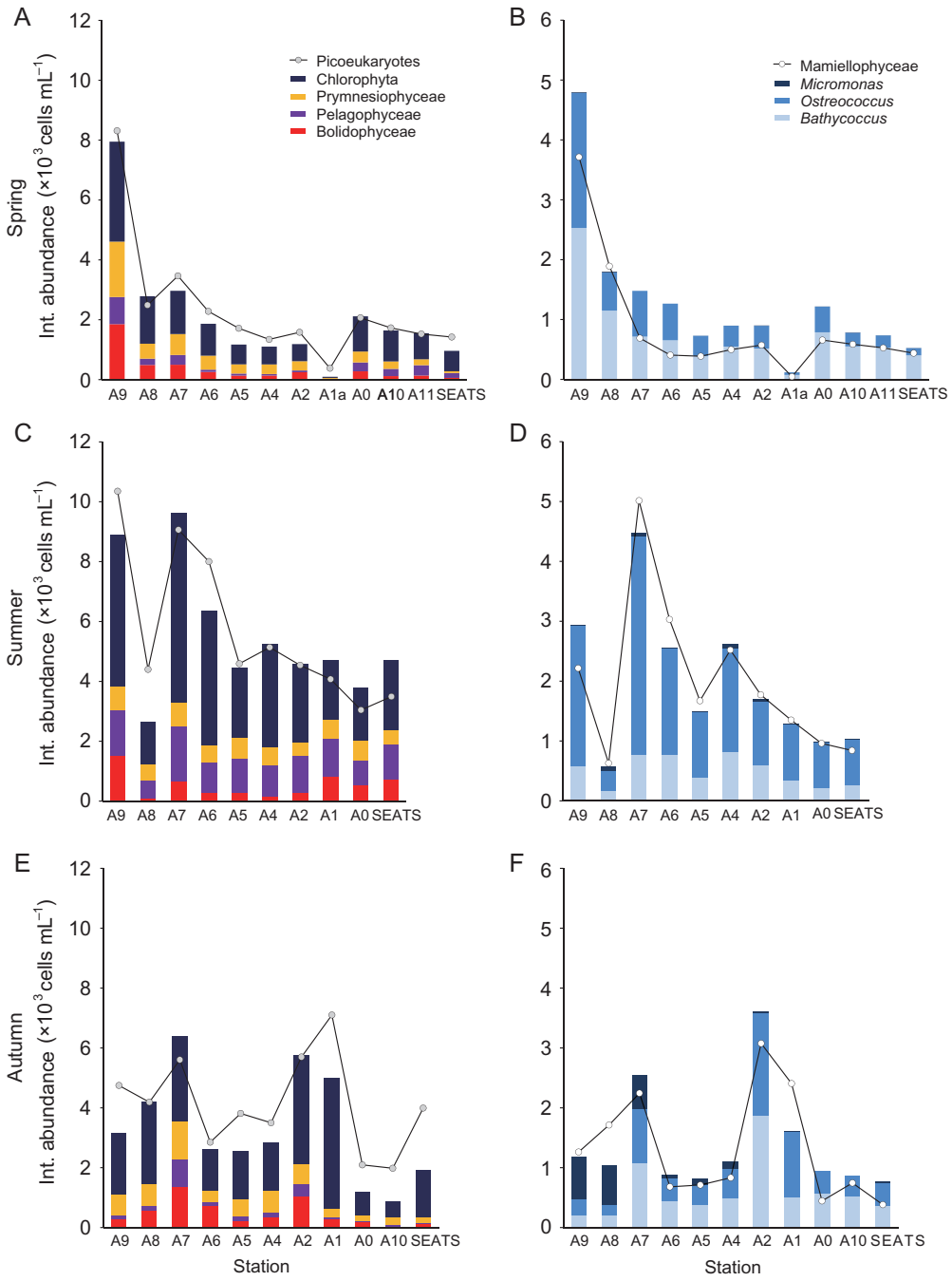

Fig. 3. Depth-integrated (Int.) abundances of picoeukaryotes, Chlorophyta, Prymnesiophyceae, Pelagophyceae, Bolidophyceae (left), Mamiellophyceae, *Micromonas*, *Ostreococcus* and *Bathycoccus* (right) (cells mL^{-1}) in the upper 150 m depth during the spring (**A**, **B**), summer (**C**, **D**) and autumn (**E**, **F**) cruises.

large variations across spatial gradients (Not *et al.*, 2008; Grob *et al.*, 2011; Kirkham *et al.*, 2011a; Cabello *et al.*, 2016). However, seasonal taxonomic PPE abundances across a large spatial gradient (a transect longer than 500 km in this study) have not been addressed because of the time-consuming process and low throughput of FISH-TSA (Not *et al.*, 2004), as well as time limitations for the vessels that perform such sampling. Overall, our study provides significant insights into the spatial and seasonal distributions of the major PPE groups based on systematic surveys of the northern SCS.

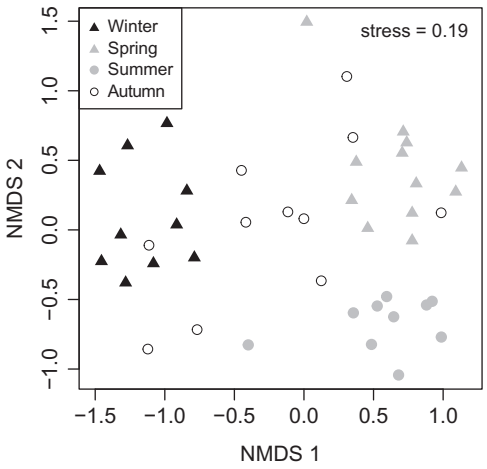

Fig. 4. NMDS diagram based on Bray–Curtis distances for the integrated abundance-based PPE assemblages at each station. Different symbols represent four different seasons (winter, black closed triangles; spring, gray closed triangles; summer, gray closed circles; autumn, open circles).

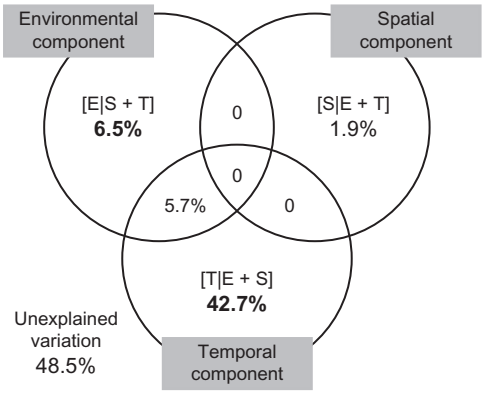

Fig. 5. Variation partitioning for the PPE assemblages tested by a three-way PERMANOVA. Pure environmental [E|S + T], pure spatial [S|E + T] and pure temporal [T|E + S] components represent the relative importance of environmental filtering, dispersal limitations and seasonality, respectively, and the shared fractions are provided. Values in bold are statistically significant based on 999 permutations ($P < 0.05$).

PPE distribution patterns in the northern SCS

Mamiellophyceae represents the most important group in the PPE assemblages in the northern SCS (Fig. 3). Our results are consistent with a recent study that used a pigment analysis and found that prasinophytes (including the class Mamiellophyceae) are an important group in the northern SCS (Ho *et al.*, 2015). Mamiellophyceae species have been observed to dominate PPE assemblages in various regions. In the English Channel and North Sea, an average of 55% of the Chlorophyta species were Mamiellophyceae, which dominated picoeukaryotic abundance (Masquelier *et al.*, 2011). At a coastal site off central Chile, Mamiellophyceae dominated PPE abundance over 2 years (Collado-Fabbri *et al.*, 2011). Overall, our results confirm that Mamiellophyceae species are the dominant group in PPE assemblages in many marine habitats, including the northern SCS.

Within the Mamiellophyceae group, our results show spatial and seasonal transitions of *Micromonas*, *Ostreococcus* and *Bathycoccus* (Fig. 3). Spatial and seasonal transitions of these three genera have been observed in several other habitats. For instance, at a coastal English Channel site, *Micromonas* was dominant in the PPE assemblages throughout the year (Not *et al.*, 2004). However, *Bathycoccus* was the major mamiellophyceaean constituent at the adjacent Helgoland Time Series Site (North Sea) (Gescher *et al.*, 2008). These two contrasting results observed in neighboring regions suggest that spatial turnover occurs among these genera. Seasonal transitions among these three genera were also observed in the northwestern Sargasso Sea, with *Micromonas* and *Ostreococcus* blooms only occurring during and immediately after the deep winter mixing period (Treusch *et al.*, 2012). Similarly, *Micromonas* only displayed considerable relative abundances in the coastal water of the northern SCS in autumn and contributed little to the Mamiellophyceae group in spring and summer, which was dominated by *Ostreococcus* and *Bathycoccus* (Fig. 3B, D and F).

Pico-sized Prymnesiophyceae species are confirmed as a key group within the PPE assemblages in the northern SCS (Figs 2AC, BC, CC, 3A, C and E). Prymnesiophyceae have been found to dominate phytoplankton Chl *a* biomass in the open ocean based on pigment analyses (Andersen *et al.*, 1996), whereas their high contributions may be primarily sustained by large-sized species (Not *et al.*, 2005). For instance, pico-sized Prymnesiophyceae species were rarely detected in the summer PPE assemblages in the North Sea, whereas nano-sized Prymnesiophyceae species can dominate in eukaryotic phytoplankton abundances (Masquelier *et al.*, 2011). Moreover, pico-sized Prymnesiophyceae have been recognized as an important PPE group in terms of biomass and abundance (Moon-van der Staay *et al.*, 2000; Liu *et al.*, 2009; Cuvelier *et al.*, 2010). Additionally, the 18S rDNA sequences of pico-sized Prymnesiophyceae have been frequently retrieved in the SCS (Wu *et al.*, 2014a), which supports our findings of their relative importance in PPE assemblages. Overall, our results reveal that pico-sized Prymnesiophyceae are distributed ubiquitously in the northern SCS and make important contributions to the PPE assemblages.

Pelagophyceae species show temporal variations with remarkably high abundances in summer in the northern

SCS (Figs 2BD and 3C); however, they are a minor PPE group in spring and autumn (Fig. 3A and E). Pelagophyceae species are key members of the PPE assemblages at the subsurface chlorophyll maximum depth. In the eastern Pacific Ocean, Pelagophyceae appeared to be a major constituent of the subsurface chlorophyll maximum community (Dupont *et al.*, 2015). Again, in the southern Pacific Ocean, Pelagophyceae species were obviously prevalent at the subsurface chlorophyll maximum depth according to a plastid 16S rDNA diversity analysis (Shi *et al.*, 2011). In the northwestern Sargasso Sea, Pelagophyceae reached annual peaks in summer when the mixed layer was shoaling and the subsurface chlorophyll maximum was well developed (Treusch *et al.*, 2012). Our findings in summer are consistent with a recent study that showed high abundances of Pelagophyceae at the subsurface chlorophyll maximum depth (Cabello *et al.*, 2016). Overall, our results confirm that Pelagophyceae tend to be more abundant at the well-developed subsurface chlorophyll maximum depth.

Bolidophyceae sporadically exhibit high abundances in different regions in the northern SCS (Fig. 2AE, BE and CE). Previous reports indicated that Bolidophyceae species were ubiquitous but contributed little to PPE assemblages (Ichinomiya *et al.*, 2016). For instance, the contributions of Bolidophyceae to the eukaryotic DNA in Mediterranean and Pacific waters were mostly lower than 1% (Guillou *et al.*, 1999). Again, Bolidophyceae were found in all water masses but always contributed <1% to the picoeukaryotic counts in the Norwegian and Barents Seas (Not *et al.*, 2005). Bolidophyceae were also believed to present a limited contribution to the biogeochemical cycles in an Arctic fjord because of their low abundances (Piwosz *et al.*, 2015). However, we observed significantly higher abundances of up to 3693 cells mL^{-1} (at a depth of 50 m at Station A2, Fig. 2CE) compared with those reported in previous studies (typically <500 cells mL^{-1}). Bolidophyceae accounted for significant fractions of the depth-integrated picoeukaryotic abundance, with values of up to 25.4% (Station A6 in autumn, Fig. 3E). Hence, we suggest that Bolidophyceae may represent important contributors to PPE assemblages in the northern SCS, although their abundances may be overestimated by including Parmales (Guillou, 2011).

Our study presents critical advantages because it provides a relatively complete view of the PPE assemblages. For example, the relative contributions of Bolidophyceae to the Chl *a* biomass could not be distinguished from that of diatoms because the same suite of pigments is observed between these two sister groups (Guillou *et al.*, 1999). Diatom-like pigment signatures in picophytoplankton may be contributed by Bolidophyceae (Not *et al.*, 2007). Our results show that the contribution of Bolidophyceae to the diatom-like pigment signatures cannot be ignored, at least in the picophytoplankton fraction. Compared with other approaches, our abundance-based analyses provide new insights into the compositional structure of PPEs.

Environmental, spatial and temporal factors that shape PPE assemblages

The seasonal distributions of PPE assemblages are differently influenced by environmental filtering, dispersal limitations and seasonality (Fig. 5). By emphasizing the metacommunity concept, we found that environmental filtering significantly accounts for the seasonal patterns of PPE assemblages, whereas dispersal limitations do not. Similar to the results of studies on phytoplankton in freshwater ecosystems (Vanormelingen *et al.*, 2008; Mazaris *et al.*, 2010; Huszar *et al.*, 2015), our results suggest that environmental heterogeneity rather than geographic distance is closely related to phytoplankton community variations. These findings are consistent with those of other studies in which microbial communities were shown to be individually structured by the environment (Van der Gucht *et al.*, 2007; Logue and Lindström, 2008). However, the pure fraction of environmental factors (6.5%) is relatively low because phytoplankton distributions are driven to a great extent by environmental variability (e.g. nutrients, Tilman *et al.*, 1982; temperature and light, Edwards *et al.*, 2016). One possible explanation for the low fraction is that certain important variables may not be considered. In addition to the environmental variables used here (Supplementary Fig. S1), many parameters, such as grazer and viral impacts, show crucial effects on PPE distributions (Pasulka *et al.*, 2015). Alternatively, the environment–abundance relationship may be weakened by the diverse ecotypes within each PPE group. For instance, *Micromonas* 18S rRNA gene sequences belonging to different phylogenetic clades were repeatedly retrieved from the SCS (Wu *et al.*, 2014a, b). The *Micromonas* abundances can be contributed by distinct clades that may respond differently to environmental variability because of niche partitioning (Foulon *et al.*, 2008). Thus, representative cultures must be established to detail the niches of these clades; however, only one culture of *Micromonas pusilla* SCSH14 has been isolated thus far (accession number KJ010081 in the 18S rDNA sequence in the GenBank database). In addition, two differently photoadapted ecotypes of *Ostreococcus* have been found to drive the global distribution patterns of this genus (Demir-Hilton *et al.*, 2011), and the occurrence of ecotype diversity in *Bathycoccus* has also been recently reported (Simmons *et al.*, 2016).

We found that spatial factors do not significantly explain the seasonal PPE assemblages, which is consistent with the hypothesis that microorganisms have great dispersal potential (Finlay, 2002; Fenchel and Finlay, 2004). Thus, the PPE dispersal rates at the spatial scale in our study were not sufficiently limited to suggest that they have a significant effect on the spatial component, although reports have indicated that microorganisms are not freely dispersed (Vyverman *et al.*, 2007; Hanson *et al.*, 2012). We suggest that active currents in the northern SCS (Hu *et al.*, 2000) promote the dispersal of PPEs in this interconnected system.

Remarkably, our findings reveal that PPE assemblages respond intensely to seasonality in the northern SCS and that the temporal component constitutes a large fraction of this seasonality (Fig. 5). PPE compositions have been found to exhibit considerable seasonal shifts caused by a number of factors related to seasonality (Not *et al.*, 2004; Collado-Fabbri *et al.*, 2011). We suggest that the observed temporal component may have been caused by seasonal factors that have not been considered. For instance, seasonal variations in microzooplankton grazing contribute to PPE distributions via top-down controls (Guo *et al.*, 2014). Moreover, trace elements (e.g. Fe and Al) from seasonal atmospheric inputs (e.g. Asian dust deposition, Maki *et al.*, 2011) are also related to PPE distributions (Marañón *et al.*, 2010), indicating that the temporal component can be partially attributed to environmental variability (a potential source of the low environmental component fraction). Altogether, this study provides important insights into the spatial and seasonal distributions of PPE assemblages in the northern SCS as well as the underlying assembly mechanisms.

SUPPLEMENTARY DATA

Supplementary data are available at *Journal of Plankton Research* online.

ACKNOWLEDGEMENT

We thank the chief scientist M. Dai and the crew of the R/V *Dongfanghong 2* for organizing the cruises and assisting with the sampling. We also thank J. Gao for her assistance with English.

FUNDING

National Key Research and Development Program (No. 2016YFA0601201); the National Natural Science Foundation of China (Nos. 41330961 and 41406158); the Doctoral Fund of the Ministry of Education of China (No. 20130121110031); the Special Fund of the State Oceanic Administration of the People's Republic of China (Nos. GASI-03-01-02-03 and 201305027).

REFERENCES

Andersen, R. A., Bidigare, R. R., Keller, M. D. and Latasa, M. (1996) A comparison of HPLC pigment signatures and electron microscopic observations for oligotrophic waters of the North Atlantic and Pacific Oceans. *Deep Sea Res. II*, **43**, 517–537.

Biegala, I. C., Not, F., Vaulot, D. and Simon, N. (2003) Quantitative assessment of picoeukaryotes in the natural environment by using taxon-specific oligonucleotide probes in association with tyramide signal amplification-fluorescence in situ hybridization and flow cytometry. *Appl. Environ. Microbiol.*, **69**, 5519–5529.

Blanchot, J., André, J.-M., Navarette, C., Neveux, J. and Radenac, M.-H. (2001) Picophytoplankton in the equatorial Pacific: vertical distributions in the warm pool and in the high nutrient low chlorophyll conditions. *Deep Sea Res. I*, **48**, 297–314.

Bonachela, J. A., Klausmeier, C. A., Edwards, K. F., Litchman, E. and Levin, S. A. (2016) The role of phytoplankton diversity in the emergent oceanic stoichiometry. *J. Plankton Res.*, **38**, 1021–1035.

Bouman, H. A., Lepère, C., Scanlan, D. J. and Osvaldo, U. (2012) Phytoplankton community structure in a high-nutrient, low-chlorophyll region of the eastern Pacific Subantarctic region during winter-mixed and summer-stratified conditions. *Deep Sea Res. I*, **69**, 1–11.

Cabello, A. M., Latasa, M., Forn, I., Morán, X. A. G. and Massana, R. (2016) Vertical distribution of major photosynthetic picoeukaryotic groups in stratified marine waters. *Environ. Microbiol.*, **18**, 1578–1590.

Collado-Fabbri, S., Vaulot, D. and Ulloa, O. (2011) Structure and seasonal dynamics of the eukaryotic picophytoplankton community in a wind-driven coastal upwelling ecosystem. *Limnol. Oceanogr.*, **56**, 2334–2346.

Cuvelier, M. L., Allen, A. E., Monier, A., McCrow, J. P., Messié, M., Tringe, S. G., Woyke, T., Welsh, R. M. *et al.* (2010) Targeted metagenomics and ecology of globally important uncultured eukaryotic phytoplankton. *Proc. Natl. Acad. Sci. USA*, **107**, 14679–14684.

De Bie, T., De Meester, L., Brendonck, L., Martens, K., Goddeeris, B., Ercken, D., Hampel, H., Denys, L. *et al.* (2012) Body size and dispersal mode as key traits determining metacommunity structure of aquatic organisms. *Ecol. Lett.*, **15**, 740–747.

Demir-Hilton, E., Sudek, S., Cuvelier, M. L., Gentemann, C. L., Zehr, J. P. and Worden, A. Z. (2011) Global distribution patterns of distinct clades of the photosynthetic picoeukaryote *Ostreococcus*. *ISME J.*, **5**, 1095–1107.

Du, C., Liu, Z., Dai, M., Kao, S.-J., Cao, Z., Zhang, Y., Huang, T., Wang, L. *et al.* (2013) Impact of the Kuroshio intrusion on the nutrient inventory in the upper northern South China Sea: insights from an isopycnal mixing model. *Biogeosciences*, **10**, 6419–6432.

Dupont, C. L., McCrow, J. P., Valas, R., Moustafa, A., Walworth, N., Goodenough, U., Roth, R., Hogle, S. L. *et al.* (2015) Genomes and gene expression across light and productivity gradients in eastern subtropical Pacific microbial communities. *ISME J.*, **9**, 1076–1092.

Edwards, K. F., Thomas, M. K., Klausmeier, C. A. and Litchman, E. (2016) Phytoplankton growth and the interaction of light and temperature: A synthesis at the species and community level. *Limnol. Oceanogr.*, **61**, 1232–1244.

Fenchel, T. and Finlay, B. J. (2004) The ubiquity of small species: patterns of local and global diversity. *Bioscience*, **54**, 777–784.

Finlay, B. J. (2002) Global dispersal of free-living microbial eukaryote species. *Science*, **296**, 1061–1063.

Foulon, E., Not, F., Jalabert, F., Cariou, T., Massana, R. and Simon, N. (2008) Ecological niche partitioning in the picoplanktonic green alga *Micromonas pusilla*: evidence from environmental surveys using phylogenetic probes. *Environ. Microbiol.*, **10**, 2433–2443.

Fuller, N. J., Campbell, C., Allen, D. J., Pitt, F. D., Zwirglmaier, K., Le Gall, F., Vaulot, D. and Scanlan, D. J. (2006a) Analysis of photosynthetic picoeukaryote diversity at open ocean sites in the Arabian Sea using a PCR biased towards marine algal plastids. *Aquat. Microb. Ecol.*, **43**, 79–93.

Fuller, N. J., Tarran, G. A., Cummings, D. G., Woodward, E. M. S., Orcutt, K. M., Yallop, M., Le Gall, F. and Scanlan, D. J. (2006b) Molecular analysis of photosynthetic picoeukaryote community structure along an Arabian Sea transect. *Limnol. Oceanogr.*, **51**, 2502–2514.

Gescher, C., Metfies, K., Frickenhaus, S., Knefelkamp, B., Wiltshire, K. H. and Medlin, L. K. (2008) Feasibility of assessing the community composition of prasinophytes at the Helgoland roads sampling site with a DNA microarray. *Appl. Environ. Microbiol.*, **74**, 5305–5316.

Giovannoni, S. J., DeLong, E. F., Olsen, G. J. and Pace, N. R. (1988) Phylogenetic group-specific oligodeoxynucleotide probes for identification of single microbial cells. *J. Bacteriol.*, **170**, 720–726.

Grob, C., Hartmann, M., Zubkov, M. V. and Scanlan, D. J. (2011) Invariable biomass-specific primary production of taxonomically discrete picoeukaryote groups across the Atlantic Ocean. *Environ. Microbiol.*, **13**, 3266–3274.

Grob, C., Ulloa, O., Li, W., Alarcón, G., Fukasawa, M. and Watanabe, S. (2007) Picoplankton abundance and biomass across the eastern South Pacific Ocean along latitude 32.5°S. *Mar. Ecol. Prog. Ser.*, **332**, 53–62.

Guillou, L. (2011) Characterization of the Parmales: much more than the resolution of a taxonomic enigma. *J. Phycol.*, **47**, 2–4.

Guillou, L., Moon-van der Staay, S. Y., Claustre, H., Partensky, F. and Vaulot, D. (1999) Diversity and abundance of Bolidophyceae (Heterokonta) in two oceanic regions. *Appl. Environ. Microbiol.*, **65**, 4528–4536.

Guo, C., Liu, H., Zheng, L., Song, S., Chen, B. and Huang, B. (2014) Seasonal and spatial patterns of picophytoplankton growth, grazing and distribution in the East China Sea. *Biogeosciences*, **11**, 1847–1862.

Hamilton, A. K., Lovejoy, C., Galand, P. E. and Ingram, R. G. (2008) Water masses and biogeography of picoeukaryote assemblages in a cold hydrographically complex system. *Limnol. Oceanogr.*, **53**, 922–935.

Hanson, C. A., Fuhrman, J. A., Horner-Devine, M. C. and Martiny, J. B. H. (2012) Beyond biogeographic patterns: processes shaping the microbial landscape. *Nat. Rev. Microbiol.*, **10**, 497–506.

Hartmann, M., Grob, C., Tarran, G. A., Martin, A. P., Burkill, P. H., Scanlan, D. J. and Zubkov, M. V. (2012) Mixotrophic basis of Atlantic oligotrophic ecosystems. *Proc. Natl. Acad. Sci. USA*, **109**, 5756–5760.

Ho, T.-Y., Pan, X., Yang, H.-H., George, T. F. W. and Shiah, F.-K. (2015) Controls on temporal and spatial variations of phytoplankton pigment distribution in the Northern South China Sea. *Deep Sea Res. II*, **117**, 65–85.

Hu, J., Kawamura, H., Hong, H. and Qi, Y. (2000) A review on the currents in the South China Sea: seasonal circulation, South China Sea warm current and Kuroshio intrusion. *J. Oceanogr.*, **56**, 607–624.

Huszar, V. L. M., Nabout, J. C., Appel, M. O., Santos, J. B. O., Abe, D. S. and Silva, L. H. S. (2015) Environmental and not spatial processes (directional and non-directional) shape the phytoplankton composition and functional groups in a large subtropical river basin. *J. Plankton Res.*, **37**, 1190–1200.

Ichinomiya, M., dos Santos, A. L., Gourvil, P., Yoshikawa, S., Kamiya, M., Ohki, K., Audic, S., de Vargas, C. *et al.* (2016) Diversity and oceanic distribution of the Parmales (Bolidophyceae), a picoplanktonic group closely related to diatoms. *ISME J.*, **10**, 2419–2434.

Jardillier, L., Zubkov, M. V., Pearman, J. and Scanlan, D. J. (2010) Significant CO_2 fixation by small prymnesiophytes in the subtropical and tropical northeast Atlantic Ocean. *ISME J.*, **4**, 1180–1192.

Kirkham, A. R., Jardillier, L. E., Holland, R., Zubkov, M. V. and Scanlan, D. J. (2011a) Analysis of photosynthetic picoeukaryote community structure along an extended Ellett Line transect in the northern North Atlantic reveals a dominance of novel prymnesiophyte and prasinophyte phylotypes. *Deep Sea Res. I*, **58**, 733–744.

Kirkham, A. R., Jardillier, L. E., Tiganescu, A., Pearman, J., Zubkov, M. V. and Scanlan, D. J. (2011b) Basin-scale distribution patterns of photosynthetic picoeukaryotes along an Atlantic Meridional Transect. *Environ. Microbiol.*, **13**, 975–990.

Kirkham, A. R., Lepère, C., Jardillier, L. E., Not, F., Bouman, H., Mead, A. and Scanlan, D. J. (2013) A global perspective on marine photosynthetic picoeukaryote community structure. *ISME J.*, **7**, 922–936.

Legendre, P. (2008) Studying beta diversity: ecological variation partitioning by multiple regression and canonical analysis. *J. Plant Ecol.*, **1**, 3–8.

Legendre, P., Borcard, D., Blanchet, F. G. and Dray, S. (2013) PCNM: MEM Spatial Eigenfunction and Principal Coordinate Analyses. R package version 2.1-2/r109. http://R-Forge.R-project.org/projects/sedar/.

Leibold, M. A., Holyoak, M., Mouquet, N., Amarasekare, P., Chase, J. M., Hoopes, M. F., Holt, R. D., Shurin, J. B. *et al.* (2004) The metacommunity concept: a framework for multi-scale community ecology. *Ecol. Lett.*, **7**, 601–613.

Lepère, C., Vaulot, D. and Scanlan, D. J. (2009) Photosynthetic picoeukaryote community structure in the South East Pacific Ocean encompassing the most oligotrophic waters on Earth. *Environ. Microbiol.*, **11**, 3105–3117.

Li, W. K. W. (1994) Primary production of prochlorophytes, cyanobacteria, and eucaryotic ultraphytoplankton: measurements from flow cytometric sorting. *Limnol. Oceanogr.*, **39**, 169–175.

Liu, H., Probert, I., Uitz, J., Claustre, H., Aris-Brosou, S., Frada, M., Not, F. and de Vargas, C. (2009) Extreme diversity in noncalcifying haptophytes explains a major pigment paradox in open oceans. *Proc. Natl. Acad. Sci. USA*, **106**, 12803–12808.

Logue, J. B. and Lindström, E. S. (2008) Biogeography of bacterioplankton in inland waters. *Freshw. Rev.*, **1**, 99–114.

Maki, T., Ishikawa, A., Kobayashi, F., Kakikawa, M., Aoki, K., Mastunaga, T., Hasegawa, H. and Iwasaka, Y. (2011) Effects of Asian

dust (KOSA) deposition event on bacterial and microalgal communities in the Pacific Ocean. *Asian J. Atmos. Environ.*, **5**, 157–163.

Marañón, E., Fernández, A., Mouriño-Carballido, B., Martínez-García, S., Teira, E., Cermeño, P., Chouciño, P., Huete-Ortega, M. *et al.* (2010) Degree of oligotrophy controls the response of microbial plankton to Saharan dust. *Limnol. Oceanogr.*, **55**, 2339–2352.

Marie, D., Shi, X. L., Rigaut-Jalabert, F. and Vaulot, D. (2010) Use of flow cytometric sorting to better assess the diversity of small photosynthetic eukaryotes in the English Channel. *FEMS Microbiol. Ecol.*, **72**, 165–178.

Masquelier, S., Foulon, E., Jouenne, F., Ferréol, M., Brussaard, C. P. D. and Vaulot, D. (2011) Distribution of eukaryotic plankton in the English Channel and the North Sea in summer. *J. Sea Res.*, **66**, 111–122.

Mazaris, A. D., Moustaka-Gouni, M., Michaloudi, E. and Bobori, D. C. (2010) Biogeographical patterns of freshwater micro- and macroorganisms: a comparison between phytoplankton, zooplankton and fish in the eastern Mediterranean. *J. Biogeogr.*, **37**, 1341–1351.

McArdle, B. H. and Anderson, M. J. (2001) Fitting multivariate models to community data: a comment on distance-based redundancy analysis. *Ecology*, **82**, 290–297.

McKie-Krisberg, Z. M. and Sanders, R. W. (2014) Phagotrophy by the picoeukaryotic green alga *Micromonas*: implications for Arctic Oceans. *ISME J.*, **8**, 1953–1961.

Millie, D. F., Paerl, H. W. and Hurley, J. P. (1993) Microalgal pigment assessments using high-performance liquid chromatography: a synopsis of organismal and ecological applications. *Can. J. Fish. Aquat. Sci.*, **50**, 2513–2527.

Moon-van der Staay, S. Y., De Wachter, R. and Vaulot, D. (2001) Oceanic 18S rDNA sequences from picoplankton reveal unsuspected eukaryotic diversity. *Nature*, **409**, 607–610.

Moon-van der Staay, S. Y., van der Staay, G. W. M., Guillou, L., Vaulot, D., Claustre, H. and Medlin, L. K. (2000) Abundance and diversity of prymnesiophytes in the picoplankton community from the equatorial Pacific Ocean inferred from 18S rDNA sequences. *Limnol. Oceanogr.*, **45**, 98–109.

Morán, X. (2007) Annual cycle of picophytoplankton photosynthesis and growth rates in a temperate coastal ecosystem: a major contribution to carbon fluxes. *Aquat. Microb. Ecol.*, **49**, 267–279.

Mouriño-Carballido, B., Hojas, E., Cermeño, P., Chouciño, P., Fernández-Castro, B., Latasa, M., Marañón, E., Morán, X. A. G. *et al.* (2016) Nutrient supply controls picoplankton community structure during three contrasting seasons in the northwestern Mediterranean Sea. *Mar. Ecol. Prog. Ser.*, **543**, 1–19.

Not, F., Latasa, M., Marie, D., Cariou, T., Vaulot, D. and Simon, N. (2004) A single species, *Micromonas pusilla* (Prasinophyceae), dominates the eukaryotic picoplankton in the Western English Channel. *Appl. Environ. Microbiol.*, **70**, 4064–4072.

Not, F., Latasa, M., Scharek, R., Viprey, M., Karleskind, P., Balagué, V., Ontoria-Oviedo, I., Cumino, A. *et al.* (2008) Protistan assemblages across the Indian Ocean, with a specific emphasis on the picoeukaryotes. *Deep Sea Res. I*, **55**, 1456–1473.

Not, F., Massana, R., Latasa, M., Marie, D., Colson, C., Eikrem, W., Pedrós-Alió, C., Vaulot, D. *et al.* (2005) Late summer community composition and abundance of photosynthetic picoeukaryotes in Norwegian and Barents seas. *Limnol. Oceanogr.*, **50**, 1677–1686.

Not, F., Simon, N., Biegala, I. and Vaulot, D. (2002) Application of fluorescent *in situ* hybridization coupled with tyramide signal amplification (FISH-TSA) to assess eukaryotic picoplankton composition. *Aquat. Microb. Ecol.*, **28**, 157–166.

Not, F., Zapata, M., Pazos, Y., Campaña, E., Doval, M. and Rodríguez, F. (2007) Size-fractionated phytoplankton diversity in the NW Iberian coast: a combination of microscopic, pigment and molecular analyses. *Aquat. Microb. Ecol.*, **49**, 255–265.

Oksanen, J., Blanchet, F. G., Kindt, R., Legendre, P., Minchin, P. R., O'Hara, R. B., Simpson, G. L., Solymos, P. *et al.* (2014) Vegan: Community Ecology Package. R Package Version 2.2-0. http://CRAN.R-project.org/package=vegan/.

Pasulka, A. L., Samo, T. J. and Landry, M. R. (2015) Grazer and viral impacts on microbial growth and mortality in the southern California Current Ecosystem. *J. Plankton Res.*, **37**, 320–336.

Piwosz, K., Spich, K., Całkiewicz, J., Weydmann, A., Kubiszyn, A. M. and Wiktor, J. M. (2015) Distribution of small phytoflagellates along an Arctic fjord transect. *Environ. Microbiol.*, **17**, 2393–2406.

R Core Team. (2014) R: A Language and Environment for Statistical Computing. R Foundation for Statistical Computing, Vienna, Austria. http://www.R-project.org/.

Schlitzer, R. (2011) Ocena Data View. http://odv.awi.de/.

Shi, X. L., Lepère, C., Scanlan, D. J. and Vaulot, D. (2011) Plastid 16S rRNA gene diversity among eukaryotic picophytoplankton sorted by flow cytometry from the South Pacific Ocean. *PLoS One*, **6**, e18979.

Shi, X. L., Marie, D., Jardillier, L., Scanlan, D. J. and Vaulot, D. (2009) Groups without cultured representatives dominate eukaryotic picophytoplankton in the oligotrophic South East Pacific Ocean. *PLoS One*, **4**, e7657.

Simmons, M. P., Sudek, S., Monier, A., Limardo, A. J., Jimenez, V., Perle, C. R., Elrod, V. A., Pennington, J. T. *et al.* (2016) Abundance and biogeography of picoprasinophyte ecotypes and other phytoplankton in the eastern North Pacific Ocean. *Appl. Environ. Microbiol.*, **82**, 1693–1705.

Simon, N., Campbell, L., Ornolfsdottir, E., Groben, R., Guillou, L., Lange, M. and Medlin, L. K. (2000) Oligonucleotide probes for the identification of three algal groups by dot blot and fluorescent whole-cell hybridization. *J. Eukaryot. Microbiol.*, **47**, 76–84.

Simon, N., LeBot, N., Marie, D., Partensky, F. and Vaulot, D. (1995) Fluorescent *in situ* hybridization with rRNA-targeted oligonucleotide probes to identify small phytoplankton by flow cytometry. *Appl. Environ. Microbiol.*, **61**, 2506–2513.

Tilman, D., Kilham, S. S. and Kilham, P. (1982) Phytoplankton community ecology: the role of limiting nutrients. *Annu. Rev. Ecol. Syst.*, **13**, 349–372.

Treusch, A. H., Demir-Hilton, E., Vergin, K. L., Worden, A. Z., Carlson, C. A., Donatz, M. G., Burton, R. M. and Giovannoni, S. J. (2012) Phytoplankton distribution patterns in the northwestern Sargasso Sea revealed by small subunit rRNA genes from plastids. *ISME J.*, **6**, 481–492.

Van der Gucht, K., Cottenie, K., Muylaert, K., Vloemans, N., Cousin, S., Declerck, S., Jeppesen, E., Conde-Porcuna, J. *et al.* (2007) The power of species sorting: local factors drive bacterial community composition over a wide range of spatial scales. *Proc. Natl. Acad. Sci. USA*, **104**, 20404–20409.

Vanormelingen, P., Cottenie, K., Michels, E., Muylaert, K., Vyverman, W. and De Meester, L. (2008) The relative importance of dispersal and local processes in structuring phytoplankton communities in a set of highly interconnected ponds. *Freshw. Biol.*, **58**, 2170–2183.

Vaulot, D., Eikrem, W., Viprey, M. and Moreau, H. (2008) The diversity of small eukaryotic phytoplankton (≤3 μm) in marine ecosystems. *FEMS Microbiol. Rev.*, **32**, 795–820.

Vyverman, W., Verleyen, E., Sabbe, K., Vanhoutte, K., Sterken, M., Hodgson, D. A., Mann, D. G., Juggins, S. *et al.* (2007) Historical processes constrain patterns in global diatom diversity. *Ecology*, **88**, 1924–1931.

Worden, A. Z., Nolan, J. K. and Palenik, B. (2004) Assessing the dynamics and ecology of marine picophytoplankton: the importance of the eukaryotic component. *Limnol. Oceanogr.*, **49**, 168–179.

Wu, W., Huang, B., Liao, Y. and Sun, P. (2014a) Picoeukaryotic diversity and distribution in the subtropical-tropical South China Sea. *FEMS Microbiol. Ecol.*, **89**, 563–579.

Wu, W., Huang, B. and Zhong, C. (2014b) Photosynthetic picoeukaryote assemblages in the South China Sea from the Pearl River estuary to the SEATS station. *Aquat. Microb. Ecol.*, **71**, 271–284.

Yeh, Y.-C., Peres-Neto, P. R., Hunag, S.-W., Lai, Y.-C., Tu, C.-Y., Shiah, F.-K., Gong, G.-C. and Hsieh, C.-H. (2015) Determinism of bacterial metacommunity dynamics in the southern East China Sea varies depending on hydrography. *Ecography*, **38**, 198–212.

Zubkov, M. V. and Tarran, G. A. (2008) High bacterivory by the smallest phytoplankton in the North Atlantic Ocean. *Nature*, **455**, 224–226.